Available online at www.sciencedirect.com

ScienceDirect

Procedia Structural Integrity 23 (2019) 191–196

Structural Integrity Procedia

www.elsevier.com/locate/procedia

9th International Conference on Materials Structure and Micromechanics of Fracture

Fatigue properties of B1914 superalloy at high temperatures

Vít Horník[a,b,*], Stanislava Fintová[a,c], Miroslav Šmíd[a], Pavel Hutař[a,c], Karel Hrbáček[d], Ludvík Kunz[a]

[a]*Institute of Physics of Materials, AS CR, Žižkova 22, Brno, 616 62, Czech Republic*
[b]*Brno University of Technology, Technická 2896/2, Brno 616 69, Czech Republic*
[c]*CEITEC IPM, Žižkova 22, Brno, 616 62, Czech Republic*
[d]*PBS Velká Bíteš, a. s., Vlkovská 279, Velká Bíteš, 595 12, Czech Republic*

Abstract

B1914 is a nickel-based superalloy with an increased amount of B (boron) and C (carbon) to reach an adequate amount of borides and carbides in the cast structure ensuring improved creep properties. However, the influence of the structure on the material high-cycle fatigue properties is not sufficiently described. The present study brings the experimental results on the high-cycle fatigue properties of a cast polycrystalline nickel-based boron-rich B1914 superalloy, obtained at temperatures of 800, 900 and 950 °C. The cast superalloy was processed by hot isostatic pressing (HIP) to diminish the casting defects. The fatigue tests were performed in symmetrical loading in laboratory air. The fracture surfaces of the specimens were studied by scanning electron microscopy in order to describe the influence of temperature on the fatigue crack initiation and propagation. Change of the primary fatigue crack propagation mechanism from the crystallographic to the non-crystallographic mechanism was observed with increasing temperature. Decrease of a material lifetime and decrease of the fatigue endurance limit due to the increasing testing temperature was observed.

Keywords: high-cycle fatigue; superalloy; B1914; high temperature.

* Corresponding author.
E-mail address: hornik@ipm.cz

10.1016/j.prostr.2020.01.085

1. Introduction

Cast polycrystalline Ni-based superalloys are an advanced group of materials with good high-temperature strength and oxidation resistance. These alloys are used in many high-temperature applications, e.g. energy or automotive industry. The superalloys components, for example, turbine blades and turbochargers wheels, are exposed to high-cycle fatigue loading due to high-frequency vibrations and creep loading due to centrifugal force during operation, e.g. Reed (2008). The problem of cast materials is casting defects created during the manufacturing process. The casting defects act as stress concentrators, strongly predetermining material fatigue properties, e.g. Kunz et al. (2012). Therefore, the hot isostatic pressing (HIP) procedure is usually adopted to reduce the casting defects size and to improve fatigue properties as a result.

The fatigue crack initiation and propagation can be described by crystallographic (known as stage I regime) vs. non-crystallographic (known as stage II regime). Among others, the dominance of stage I or II (alternatively mixed) crack propagation regimes are strongly influenced by the component operating temperature. In general, the transition temperatures between crystallographic and non-crystallographic crack propagation for Ni-based superalloys are in a range from 650 to 1000 °C, in dependence on the material chemical composition, structural stability, etc., e.g. Baluc and Schäublin (1996), MacLachlan and Knowles (2001), Pineau and Antolovich (2009), Šmíd et al. (2016), Šmíd et al. (b) (2016).

A special group of Ni-based superalloys with a content of interstitial elements, namely B (boron) and C (carbon) is commonly known as BC alloys. In general, the specific amount of B (more than 0.03 wt. %) and C (0.02 ÷ 0.2 wt. %) is required to ensure the boride or carbide particles precipitation in Ni-based superalloys, e.g. Xiao et al. (2005), Zhou et al. (2008). The presence of borides and carbides increase the grain boundary cohesive strength mainly, and therefore, the creep resistance increase with increasing content of these particles is observed, e.g. Zhao et al. (2016). On the other hand, it is well known that coarse particles (in the worst case a network structure) of carbides or borides on the grain boundaries serve as stress concentrators and as potential fatigue crack initiation sites, e.g. Kontis et al. (2014). Hence, the control of the alloy chemical composition and alloying elements content is very important.

The polycrystalline B1914 superalloy is a BC alloy with the lowest Mo + W + Ta + Nb content from the BC alloy group. The high content of Ti + Al elements results in a high volume fraction of γ' phase, approx. 60 %. The borides of mainly $(Mo, Cr, Ni)_3 B_2$ structure are precipitated along the grain boundaries and in the interdendritic areas, e.g. da Silva Costa et al (2014).

The B1914 superalloy has been developed over five decades ago, however, the alloy high-cycle fatigue properties at high temperatures are still missing in the open literature. The aim of this work is to determine the high-cycle fatigue properties of the B1914 superalloy at the temperatures of 800, 900 and 950 °C in fully reverse loading. Detailed fractographic analysis with the aim to identify fatigue crack initiation and fatigue crack propagation was performed. The character of the fatigue crack propagation in dependence on the testing temperature in terms of potential change from the crystallographic to the non-crystalographic fatigue crack propagation was analyzed. The obtained data were discussed in relation to the MAR-M 247 behavior published in the literature.

2. Material

The cast polycrystalline B1914 superalloy in a form of pre-cast rods was provided by PBS Velká Bíteš company. The chemical composition of the studied superalloy was following (in wt. %): 0.009 C, 0.08 B, 9.99 Cr, 9.63 Co, 5.51 Al, 5.28 Ti, 2.90 Mo, 0.002 Zr, balance Ni. The casting temperature was 1360 ± 10 °C. The pre-cast rods were processed by HIP treatment at the temperature 1155 °C and pressure 100 MPa for 3 hours in argon atmosphere followed by two steps heat treatment consisting of solution annealing at the temperature 1080 °C for 4 hours with cooling on the air and precipitation annealing at the temperature 900 °C for 10 hours with cooling on the air. The final structure of the processed B1914 superalloy is a coarse dendritic with the average of grain size of about 2.3 mm (measured by the linear intercept method on 10 different areas of the microstructure). The material structure contains γ matrix, γ' precipitates (approx. 60 % of the volume fraction), γ / γ' eutectics and numerous carbides and borides along grain boundaries and in interdendritic areas, Fig. 1. The casting defects with the size range from 150 to 800 μm were observed in the cast and HIPed structure.

The fatigue tests were performed on resonant testing machine Amsler with 100 kN force range under fully reverse load control regime. The specimens were heated to the testing temperatures of 800, 900 and 950 °C by an electric resistance furnace on air. The testing temperature was controlled by two thermocouples with accurancy of ± 1 °C. The frequency of cyclic loading was in the range of 110 ÷ 120 Hz. Cylindrical test specimens with a geometry shown in Fig. 2 were used for the purposes of this study. Gauge lengths of all specimens were mechanically ground. The fractographical analysis of fractured specimens by TESCAN Lyra3 XMU scanning electron microscope (SEM) was performed.

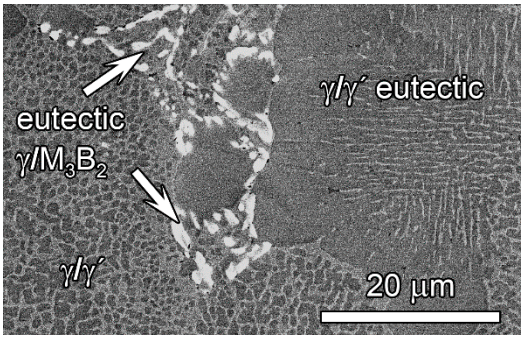

Fig. 1. Microstructure of B1914.

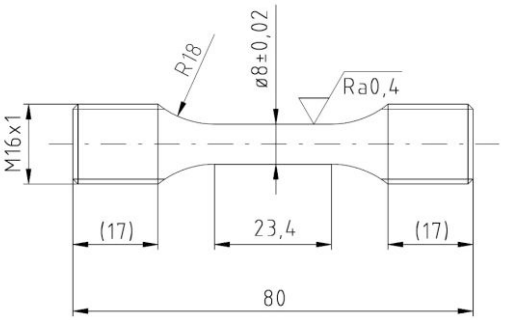

Fig.2. Fatigue specimen geometry.

3. Results and discussion

In Fig. 3 the S-N curves of B1914 superalloy for high-cycle region measured at the temperatures 800, 900 and 950 °C compared with the results of MAR-M 247 superalloy published previously by Šmíd et al. (2016) are shown. The polycrystalline MAR-M 247 superalloy investigated by Šmíd et al. (2016) was also processed by the HIP treatment reducing the size of casting defects to the size of around 400 μm. The final structure of the alloy contained about 60 % volume fraction of γ' phase. The B1914 and MAR-M 247 superalloys achieve a similar high-cycle fatigue behavior at 800 °C with relatively high scatter of experimentally determined points, see Fig. 3 (a). The fatigue endurance limit of both superalloys is 220 MPa at 800 °C. However, significant difference in the fatigue lives at the temperature of 900 °C was observed, Fig. 3 (b). The lower number of cycles to the fracture were characteristic for B1914 in the comparison with MAR-M 247 at the same stress amplitude. The fatigue endurance limit of B1914 decreased to 190 MPa at 900 °C and it is lower than the fatigue endurance limit determined for MAR-M 247. High-cycle S-N curves of B1914 and MAR-M 247 obtained at 950 °C are shown in Fig. 3 (c). Also, here superiority of MAR-M 247 was confirmed at high temperatures. Both alloys exhibited similar fatigue properties at 950 °C when compared to the properties at 900 °C.

In Fig. 4 (a) and (b) are shown the fracture surfaces of the B1914 superalloy specimens after fatigue tests at 800 °C observed by SEM. The same stress amplitude of 280 MPa in both cases was applied. The interior fatigue crack initiation from the casting defects (marked by an arrow in Fig. 4 (a) and (b)) was responsible for the fracture of the specimens. The same mechanism was characteristic for the whole spectrum of the applied stress amplitudes and the fish eye was observed on the fracture surfaces of all fractured specimens. The facets, as the sign of the crystallographical stage I crack propagation, were observed inside the fish eye around the crack initiation site on fracture surfaces of all specimens tested at 800 °C. Outside of the fish eye area, the fatigue crack propagation was entirely non-crystallographic in stage II regime, perpendicular to the loading axis. The striations were observed in the area of the non-crystallographic crack growth. The scatter of reached number of cycles to the fracture between individual specimens was caused by the presence of casting defects. The specimen lifetime corresponds to the size of the casting defect responsible for the fatigue crack initiation. The specimen with a smaller size of defect reached a higher fatigue lifetime, see Fig. 4.

Fracture surfaces of specimens loaded at 900 °C are shown in Fig. 5. The fatigue crack initiated on the present casting defects in the specimen interior. The fatigue crack propagation in the fish eye area was in stage I and II

regime mixture. The size of facets in the created fish eyes was decreasing with increasing stress amplitudes, Fig. 5. The fatigue lifetime of individual specimens was dependent on the size of the present casting defects. The specimen with a larger fatigue crack initiating defect (435 μm, Fig. 5(a)) loaded by 210 MPa reached lower number of cycles to the fracture (1.017×10^6 cycles) when compared to the specimen fractured at higher stress amplitude (240 MPa, Fig. 5(b)) due to a smaller defect (192 μm) responsible for the fatigue crack initiation. The striations and non-crystallographic crack propagation were observed outside of the fish eye area.

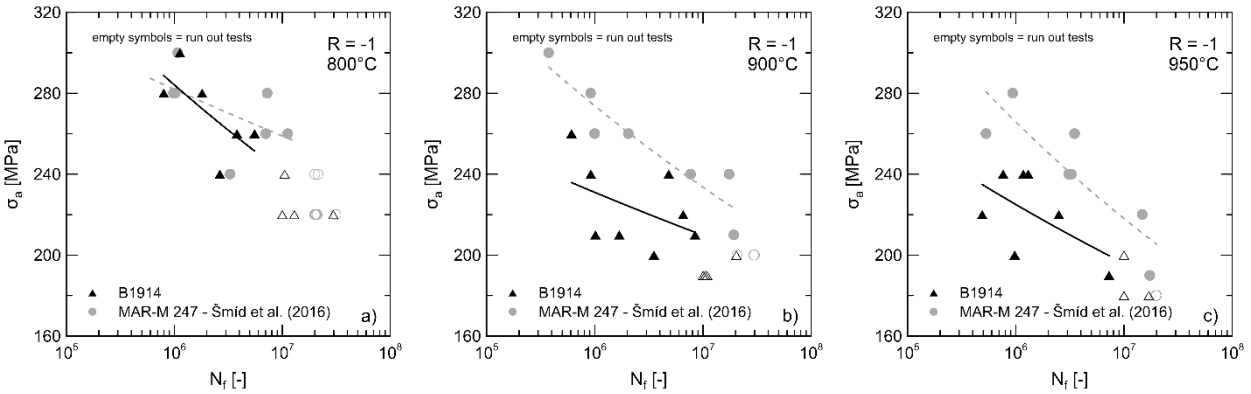

Fig. 3. High-cycle S-N curves of B1914 and reference MAR-M 247 superalloy at the temperatures of (a) 800, (b) 900 and (c) 950 °C.

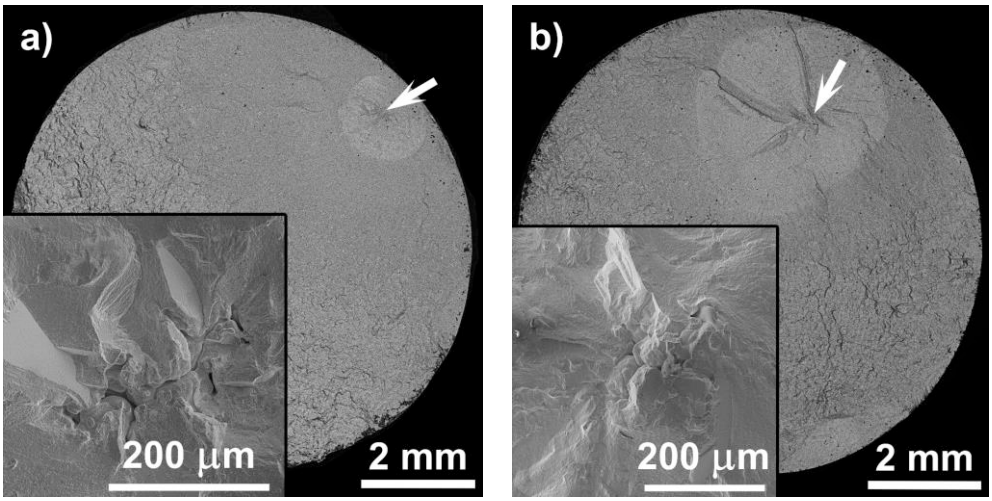

Fig. 4. Fracture surface of the B1914 superalloy specimens after cycling by 280 MPa stress amplitude at 800 °C. a) $N_f = 0.796 \times 10^6$ cycles, defect size = 275 μm; b) $N_f = 1.808 \times 10^6$ cycles, defect size = 220 μm.

Increase of the testing temperature to 950 °C resulted in the elimination of crystallographic crack propagation in stage I regime, as shown in Fig. 6. The crack initiated and propagated in stage II regime, in the direction perpendicular to the loading axis. The effect of the casting defect on the fatigue lifetime of the fractured specimens was observed, Fig. 6 (a) and (b).

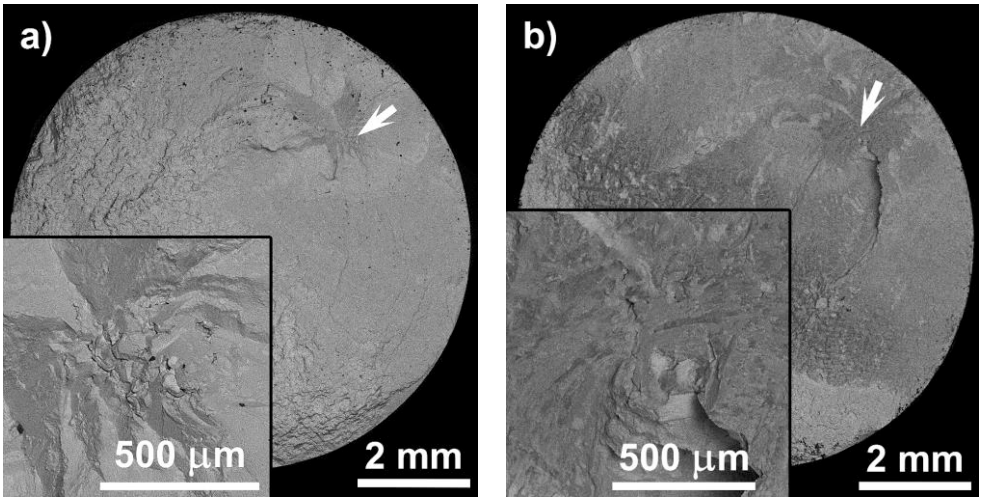

Fig. 5. Fracture surface of the specimen of B1914 superalloy after cycling at 900 °C.
a) σ_a = 210 MPa, N_f = 1.017×10^6 cycles, defect size = 435 μm; b) σ_a = 240 MPa, N_f = 4.821×10^6 cycles, defect size = 192 μm.

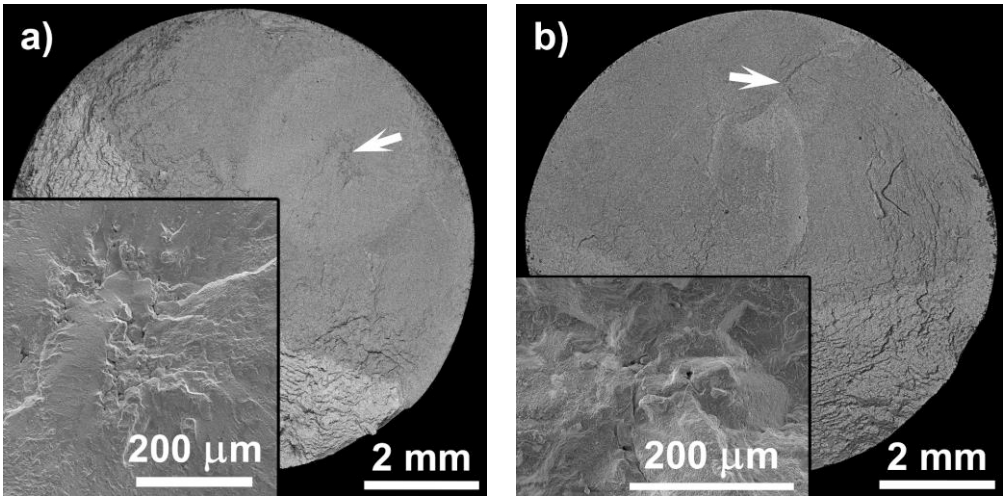

Fig. 6. Fracture surface of the B1914 superalloy specimens after cycling by 220 MPa stress amplitude at 950 °C.
a) N_f = 0.489×10^6 cycles, defect size = 750 μm; b) N_f = 2.500×10^6 cycles defect size = 160 μm.

The influence of testing temperature on crystallographic crack propagation was observed on the fracture surfaces. The largest facets were observed on the fracture surfaces of the specimens fractured at 800 °C. An increase of the testing temperature resulted in reduction of the size of facets (900 °C) or in elimination of the facets (950 °C). The crack propagation in stage I regime was observed to localize in the fish eye area only. The stage II crack propagation was observed in and outside of the fish eye, depending on the testing temperature. Stage II crack propagation becomes more significant with increasing testing temperature due to the thermally activated processes such as diffusion and climb of dislocations. This phenomenon was reported in several studies on MAR-M 247 superalloy, e.g. Šmíd et al. (2016), or other different alloys, e.g. MacLachlan and Knowles (2001), Pineau and Antolovich (2009), Baluc and Schäublin (1996).

The interior fatigue crack initiation of all specimens is given by the presence casting defects at 800, 900 and 950 °C. The scatter of the fatigue lifetime corresponds to the defect size. This is in agreement with the literature data, e.g. Kunz et al. (2012) or Pineau and Antolovich (2009). The optimization of the casting procedure or HIP

treatment should lead to suppressing the casting defects and consequently improve high-cycle fatigue properties of the material.

4. Conclusions

The high-cycle fatigue properties of B1914 (processed by HIP treatment) were experimentally determined under symmetrical cyclic loading at three different temperatures (800, 900 and 950 °C). The fatigue crack initiation occurred in the interior of all fractured specimens. The scatter of the obtained fatigue data was dependent on the casting defect size.

Stage I fatigue crack propagation which is characteristic by facets in the fish eye was observed on the fractures surface only at temperatures 800 and 900 °C. The facet size was decreasing with increasing testing temperature. Facets were not observed on the fracture surfaces of the specimens tested at 950 °C. At 950 °C, the crack was propagating in stage II regime only.

The fatigue endurance limit determined for the material tested 800 °C was 220 MPa. The decrease of the fatigue lifetime of the superalloy with the temperature increase to 900 °C was observed, however, additional testing temperature increase did not influence material behavior significantly. The fatigue endurance limit determined for the material at 900 °C was 190 MPa and for 950 °C was 180 MPa.

Acknowledgements

This research was financially supported by the project CZ.01.1.02/0.0/0.0/15_019/0002421 of Ministry of Industry and Trade of the Czech Republic and by the project of Ministry of Education, Youth and Sports of the Czech Republic m-IPMinfra (CZ.02.1.01/0.0/0.0/16_013/0001823). The base research infrastructure IPMinfra was used for the experimental work.

References

Baluc, N., Schäublin, R., 1996. Weak beam transmission electron microscopy imaging of superdislocations in ordered Ni3Al. Philosophical Magazine A 74, 113-136.

Kontis, P., Yusof, H.A.M., Moore, K.L., Grovenor, C.R.M., Reed, R.C., 2014. On the effect of boron on the mechanical properties of a new polycrystalline superalloy, 2nd European Symposium on Superalloys and their Applications. E D P Sciences, Giens, FRANCE.

Kunz, L., Lukáš, P., Konečná, R., Fintová, S., 2012. Casting defects and high temperature fatigue life of in 713LC superalloy. International Journal of Fatigue 41, 47-51.

MacLachlan, D. W., Knowles, D. M., 2001. Fatigue behaviour and lifing of two single crystal superalloys. Fatigue and Fracture of Engineering Materials and Structures. 24(8): p. 503-521.

Pineau, A., Antolovich, S.D., 2009. High temperature fatigue of nickel-base superalloys – A review with special emphasis on deformation modes and oxidation. Engineering Failure Analysis 16, 2668-2697.

Reed, R.C., 2008. The Superalloys: Fundamentals and Applications. Cambridge University Press.

da Silva Costa, A.M., Nunes, C.A., Baldan, R., Coelho, G.C., 2014. Thermodynamic Evaluation of the Phase Stability and Microstructural Characterization of a Cast B1914 Superalloy. Journal of Materials Engineering and Performance 23, 819-825

Šmíd, M., Horník, V., Hutař, P., Hrbáček K., Kunz, L., 2016. High Cycle Fatigue Damage Mechanisms of MAR-M 247 Superalloy at High Temperatures. Trans Indian Inst. Met. 69, 393 – 397.

Šmíd, M., Hutař, P., Horník, V., Hrbáček, K., Kunz, L., 2016. Stage I fatigue cracking in MAR-M 247 superalloy at elevated temperatures, 21st European Conference on Fracture, (Ecf21), pp. 3018-3025. (b)

Xiao, L., Chen, D.L., Chaturvedi, M.C., 2005. Effect of boron and carbon on the fracture toughness of IN 718 superalloy at room temperature and 650 degrees C. Journal of Materials Engineering and Performance 14, 528-538.

Zhao, Y.S., Zhang, J., Luo, Y.S., Li, J., Tang, D.Z., 2016. Effects of Hf and B on high temperature low stress creep behavior of a second generation Ni-based single crystal superalloy DD11. Materials Science and Engineering: A 672, 143-152.

Zhou, P.J., Yu, J.J., Sun, X.F., Guan, H.R., Hu, Z.Q., 2008. The role of boron on a conventional nickel-based superalloy. Materials Science and Engineering: A 491, 159-163.